EUROPHYSICS LETTERS 10 November 1995

Europhys. Lett., 32 (5), pp. 431-436 (1995)

Gravity-Induced Shape Transformations of Vesicles.

M. KRAUS, U. SEIFERT and R. LIPOWSKY

Max-Planck-Institut für Kolloid- und Grenzflächenforschung
Kantstr. 55, 14513 Teltow-Seehof, Germany
Institut für Festkörperforschung, Forschungszentrum Jülich
52425 Jülich, Germany

(received 24 May 1995; accepted in final form 22 September 1995)

PACS. 68.10-m - Fluid surfaces and fluid-fluid interfaces.
PACS. 82.70-y - Disperse systems.
PACS. 87.22Bt - Membrane and subcellular physics and structure.

Abstract. - We theoretically study the behaviour of vesicles filled with a liquid of higher density than the surrounding medium, a technique frequently used in experiments. In the presence of gravity, these vesicles sink to the bottom of the container, and eventually adhere even on non-attractive substrates. The strong size dependence of the gravitational energy makes large parts of the phase diagram accessible to experiments even for small density differences. For relatively large volume, non-axisymmetric bound shapes are explicitly calculated and shown to be stable. Osmotic deflation of such a vesicle leads back to axisymmetric shapes and, finally, to a collapsed state of the vesicle.

Lipid vesicles are simple models for many membrane-bounded compartments occurring in biology, such as cells or transport vesicles [1]. From a physical point of view, they can be understood as flexible closed surfaces whose shapes and dynamics are controlled primarily by the bending energy. Frequently, however, additional interactions are relevant for a particular experimental situation. The interactions of two vesicles have been studied with micropipet experiments [2]. Weak adhesion of a single vesicle to a substrate can be used to reduce translational and rotational diffusion and thus to facilitate data analysis [3]. In this case, one prefers a small contact area, in order to reduce effects exerted by the substrate. In other experiments, however, adhering vesicles with a large contact area serve as a model of a bound planar membrane whose fluctuations can be analysed [4-6].

In order to stabilize the vesicle at the bottom of the measurement chamber, a difference in density between the fluids inside and outside the vesicle is often employed. Mostly, this is done by solvation of different sugars with equal osmolarity, but different specific weights [3]. However, while bending and adhesion energies have been taken into account, gravitational energies have so far been neglected in the analysis of experiments [4, 3]. We will show that this is not justified even for the small density differences usually employed.

A simple scaling argument reveals that the contribution of the gravitational energy cannot be neglected for large vesicles: Whereas the curvature energy is scale invariant [7], adhesion energies behave as $F_{\mathrm{adh}} \propto R_0^2$. However, the gravitational energy scales as $F_{\mathrm{grav}} \propto R_0^4$, because it is proportional to the volume multiplied with the height of the centre of mass of the

vesicle above the substrate. Here, $R_0 \equiv (A/(4\pi))^{1/2}$ is the radius of a sphere with the same area, which sets the length scale. The energy scale is set by the bending rigidity, κ, of the membrane. We introduce the dimensionless gravity parameter

$$g \equiv \frac{g_0 \, \Delta\varrho \, R_0^4}{\kappa} , \tag{1}$$

where $g_0 \simeq 9.81 \text{ m s}^{-2}$ is the acceleration of gravity and $\Delta\varrho$ denotes the density difference between the fluids inside and outside the vesicle. Typical values for the latter are around $0.01 \ldots 0.1 \text{ g cm}^{-3}$, *i.e.* a few per cent of the density of water. Giant vesicles can reach a size of $R_0 \simeq (5\text{–}50)\,\mu\text{m}$. With $\kappa \simeq 10^{-19}\,\text{J} \simeq 25 k_B T$, one obtains values of $0.5\text{–}5 \cdot 10^4$ for g. Thus, for giant vesicles, the gravitational energy can be varied over a large range and may be of the same order of magnitude as the curvature energy.

Previous work has successfully explained the observed shapes of freely floating giant vesicles in solution by calculating shapes of minimal bending energy with given constraints [7-11]. The membrane-substrate interaction for vesicle adhesion was modelled by a contact energy W [12], which is justified on a macroscopic scale since the range of most interactions is orders of magnitude smaller than typical vesicle sizes. Our effective energy,

$$F = \frac{\kappa}{2} \int \mathrm{d}A \, (C_1 + C_2 - C_0)^2 + g \int \mathrm{d}V Z - W A_{\text{adh}} - W' A_{\text{self}} , \tag{2}$$

consists of these energies augmented by gravitational and membrane self-adhesion energies. Here, C_1 and C_2 are the principal curvatures, and C_0 denotes the spontaneous curvature of the membrane. Furthermore, Z denotes the height of a volume element above the substrate, and A_{adh} is the contact area of adhesion at the substrate. The membrane adheres to itself with a contact area A_{self} and contact energy W'.

The behaviour for very small and very large gravitational energies may be understood by simple arguments. Vesicles filled with a fluid that is only slightly denser than the surrounding fluid, *i.e.* for small g, will always touch the bottom of the measurement chamber but will not necessarily form a finite contact area. We will call this state «pinned» if the vesicle touches the wall only in a single point [13]. A contact area of finite size will be formed, as soon as the cost in bending energy which is necessary in order to form this area is balanced *globally* by a gain in gravitational energy. In the axisymmetric case, C_1 will denote the principal curvature along the contour. The criterion for the transition from the pinned state to a bound state then follows from the *local* boundary condition at the contact point S_1 of the contour [12] as given by

$$R_0 C_1(S_1) = \sqrt{2w} , \tag{3}$$

where $w \equiv W R_0^2/\kappa$. For vanishing adhesion energy, *i.e.* $w = 0$, this condition becomes $C_1(S_1) = 0$. Then, the continuous adhesion transition between the pinned state and a bound state with finite contact area happens, when g reaches a critical value where the vesicle is deformed into a shape which has vanishing mean curvature at the contact point. Varying w yields a whole line of adhesion transitions at $g = g_{\text{adh}}(w)$. Numerically, we find $g_{\text{adh}}(w = 0) \simeq$ $\simeq 0.45$ for $C_0 = 0$ without volume constraint. For $g = 0$, adhesion happens at $w = 2$ induced just by the contact potential [12].

The behaviour for large g is different from the large-w limit. In the latter limit, the bending energy may be neglected, and the vesicles will attain the shape of maximal contact area for given constraints, which is a spherical cap with a finite contact angle determined by the Young-Dupré equation [12]. In the limit of high gravitational energy, bending is also irrelevant, but now—given that the volume is fixed—the shape of least energy is that of a flat

disc, as can be seen from an expansion of the gravitational energy as a function of the reduced volume, $v \equiv V/(4R_0^3/3\pi)$, for small volumes (1).

We now want to discuss the details of the shape transformations for general g, which requires the calculation of shapes and their energies. In order to keep the number of parameters small, we introduce a few simplifications. First, we consider vanishing spontaneous curvature, *i.e.* $C_0 = 0$, assuming that the different compositions of the solutions do not affect the symmetry of the bilayer. Second, we will focus on $w = 0$ for the membrane-substrate adhesion and $w' = 0$ for the membrane self-adhesion contact energies (2). The case with $w \neq 0$ and $w' \neq 0$ will be discussed in more detail in another publication [14]. Axisymmetric shapes can be calculated numerically by solving the Euler-Lagrange equations resulting from eq. (2) with appropriate boundary conditions [10, 14]. A simple argument, however, shows that non-axisymmetric shapes are also relevant.

For large reduced volume, *i.e.* for shapes close to a sphere, free prolate vesicles have smaller energy than the corresponding discocytes [10]. When these shapes adhere under gravity, they will orient their long axis parallel to the wall. For any finite g, the vesicle will be flattened, thus giving rise to non-axisymmetric shapes. In order to conserve volume, the asphericity in the plane parallel to the wall has to be reduced. As discussed above, we expect the limit shapes for large density difference to be axisymmetric with the symmetry axis perpendicular to the wall. In general, such an axisymmetric shape should be reached asymptotically for large g. In addition, we expect a discontinuous shape transition between adhering discocytes and non-axisymmetric prolates for small g and $v \gtrsim 0.65$, since the free vesicle with $C_0 = 0$ exhibits a discontinuous transition between discocytes and prolates at $v \simeq 0.65$ [10].

In order to calculate the energy of these non-axisymmetric shapes a numerical method can be employed, which minimizes the discretized curvature energy of a triangulated surface subject to given constraints. We have used Brakke's Surface Evolver [15] program, which also allows incorporation of the gravitational energy easily. Since numerical minimization for a hard-wall constraint is more problematic than for a soft wall, we have used the latter by exposing the vesicle to the additional potential $V_w(z) = V_{0w} \exp[-Z/Z_0]$, with $V_{0w}/\kappa = 5$ and $Z_0/R_0 = 0.1$, which leads to a numerically stable algorithm and induces only minor deformation of the vesicle shape.

The Surface Evolver data shown in fig. 1 indicate a «tricritical» point at $v = v_{tr} \simeq 0.88$. Hysteresis effects indicating a discontinuous transition are found only at $v < v_{tr}$. In the limit of small g, the limit of metastability for the discocytes at $v = 0.75$ coincides with the results of an explicit stability analysis for free vesicles [16]. At the spinodals, the energy difference between the unstable and the stable shape is of the order of several $k_B T$; *e.g.*, at $v = 0.7$, $g = 11$, the energy of the prolates is $1.50\kappa \simeq 35 k_B T$ above the energy of the stable discocytes.

In the limit $v \approx 1$, *i.e.* close to the sphere, we have also calculated non-axisymmetric shapes using two simple approximations, whose results confirm the Evolver data and the existence of a continuous transition in this regime. In the first approach, we expand the curvature energy and geometrical quantities such as area, volume and centre of mass in spherical harmonics up to $l = 2$ along the lines of ref. [17]. The influence of gravity is computed under the assumption of ellipsoidal shapes, so that this method is only useful for

---

(1) The shape of a vesicle for large g can be approximated by a «coin»-shaped flat disc of fixed area $A = 4\pi R_0^2$. Denoting the gravitational part of its free energy by F_{grav}, we obtain $F_{grav}/\kappa g = 4/9\pi v^2 + \sqrt{32}/27\pi v^3 + 4/27\pi v^4 + \ldots$. This is lower than the result $F_{grav}/\kappa g = 32/27\pi v^2 + 64/729\pi v^4 + \ldots$ for the analogous spherical cap.

(2) Strictly speaking, the vesicle has non-adhesive contact with the substrate in the case $w = 0$. Keeping the generalization to $w \neq 0$ in mind, we will also call this case «adhesion».

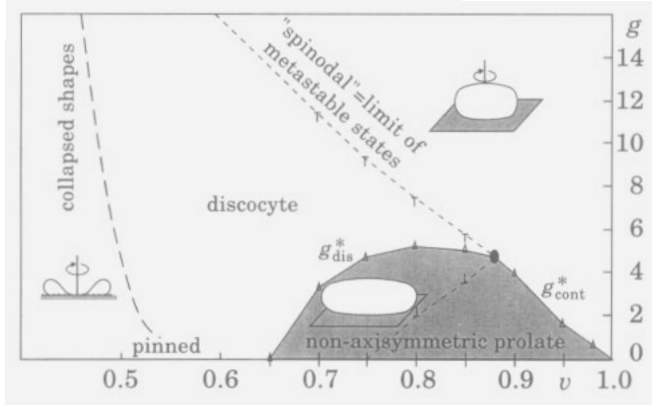

Fig. 1. – Phase diagram for adhering vesicles as a function of gravitational parameter, g, and reduced volume, v. Non-axisymmetric shapes and the large-volume transition are computed using the Surface Evolver program, while axisymmetric shapes are solutions of the Euler-Lagrange equations with $w = 0$. The transition $g^*(v)$ between the non-axisymmetric prolates and the discocytes is discontinuous for $v < v_{tr} \simeq 0.88$ (full line) and continuous for $v > v_{tr}$ (dashed) separated by a tricritical point (black dot). For the discontinuous transition, the limit curves of metastable states or spinodals are shown in the figure by dashed lines. At $g \lesssim 1$ there is an additional transition from «pinned» vesicles to those adhering in a finite area; the transition line is not shown. On the small-v side of the phase diagram, collapsed shapes become relevant.

volumes $v \gtrsim 0.98$. In the second approach, we consider the restricted set of shapes generated by ellipsoids deformed by special conformal transformations [18]. Calculation of both curvature and gravitational energies is now exact, but smaller-volume shapes are not very well described by the restricted variation. Both approximations predict a continuous symmetry-breaking transition at finite g, and give an approximation for the transition line $g^*(v)$, but fail to produce the tricritical point necessary to change to a discontinuous transition at smaller volumes. At $v \approx 1$, however, both methods predict that $g^*(v)$ goes to zero. We conclude that for large v and intermediate g there are no stable adhering prolates.

For the general case of non-zero spontaneous curvature, the phase diagram becomes more complex [14]. The trends, however, can be understood in analogy to the effect of spontaneous curvature on free vesicles [10]. Negative C_0 stabilizes bound discocytes and stomatocytes, while positive C_0 stabilizes bound prolates, and, finally, pears and budded shapes. If one expands the shapes for $g \neq 0$ around the shapes at $g = 0$, one finds that the amplitudes of the deformation depend linearly on g. The prefactors, however, are a non-monotonic function of C_0.

For small v, new phenomena occur: i) stomatocytes enter the phase diagram; ii) the self-avoidance of the membrane has to be taken into account. Free discocytes with $C_0 = 0$ self-intersect at their symmetry axis for $v = 0.515$ [10], while adhering discocytes self-intersect for v between 0.4 and 0.5, depending on g and w. The physical shapes for even smaller volumes involve membrane self-adhesion (shapes, which we denote as «collapsed» in fig. 1) even if there is no explicit membrane self-adhesion energy. For vanishing or small self-adhesion energy, the cost in bending energy for forming a finite self-adhesion area is high at the contact point, and there is a region of «self-pinned» shapes in the phase diagram. If the self-adhesion energy is large, the possibility of a first-order collapse transition arises. A shape sequence involving such a collapse transition as generated by osmotic deflation (see below) is shown in fig. 2.

For $g = 0$ and reduced volume $v \leqslant 0.45$, adhering stomatocytes are stable when the adhesion energy, w, exceeds a critical threshold value [12]. As these shapes rise higher above

the substrate than the discocytes of equal volume, they will not be stable for large g. With increasing g, adhering stomatocytes redistribute their volume towards the substrate. As a consequence, the neck at the top of the vesicle closes. For all membrane self-adhesion energies $w' > 0$, we find a discontinuous self-adhesion transition. At the top of the vesicle, a finite area around the infinitesimal neck then sticks together. The detailed order and sequence of the transitions between collapsed and non-collapsed, free and adhering stomatocytes/discocytes in the small-volume regime depends crucially on the values of w and w' and will be discussed elsewhere [14]. The energy diagram and shape sequence of a trajectory with fixed g is shown in fig. 3. The phase diagram might involve even more complicated shapes such as self-adhering non-axisymmetric shapes or shapes that self-adhere in more than one place. This should be kept in mind when one tries to understand the conformation of swollen lipid and vesicle-like structures emerging near a substrate. Many conformations formerly ascribed to defects in the membrane might be stable states of pure lipid membranes involving self-adhesion.

There are several possibilities for experimentally scanning the phase diagram with a single vesicle. Raising the temperature will expand the membrane much more than the liquid. In this case, the actual volume and the density difference remain constant, but the reduced volume, v, will decrease, while g will increase because of its dependence on R_0. A trajectory starting at a point $(g, v) = (g_s, v_s)$ will thus continue as $g(v) = g_s (v_s/v)^{4/3}$.

Alternatively, one may vary the volume by exchanging the sugar concentration, X_{ex}, of the exterior fluid, while keeping the number of dissolved osmotically active particles inside the vesicle, $N_{in} = VX_{in}$, constant. The volume will then adjust in such a way that the osmotic pres-

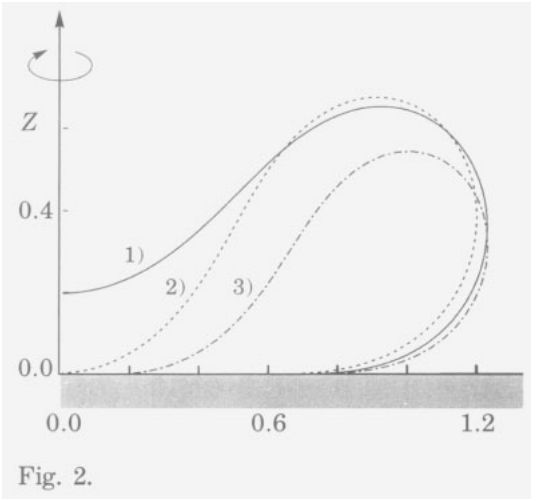

Fig. 2.

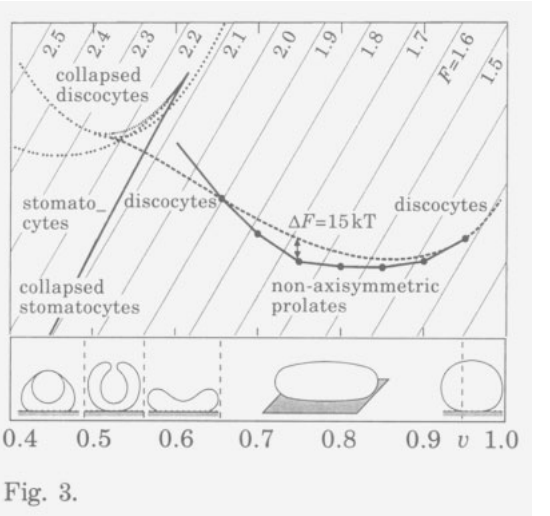

Fig. 3.

Fig. 2. – Sequence of shapes for collapse transition of discocytes. Shapes are taken from a typical osmotic trajectory generated by varying the sugar content of the exterior fluid (eq. (4)). Parameters approximately matching a typical experimental situation [4] with $R_0 \simeq 5\,\mu m$ and concentrations of the order 100 mM sucrose or glucose are: $w = w' = 0$, $N_{in} = 10^{11}$, $g_0 R_0 m_{in}/\kappa = 10^{-10}$, $m_{ex} = 0.5 m_{in}$, $X_{ext} R_0^3 \simeq 4.3 \cdot 10^{-10}$ (1)) $4.8 \cdot 10^{-10}$ (2)), and $6.3 \cdot 10^{-10}$ (3)), leading to volumes $v = 0.555$ (1)), $v = 0.500$ (2)), and $v = 0.379$ (3)), respectively.

Fig. 3. – Energy F for adhering vesicles at $g = 2$, $w = 0$, and $w' = 0.05$ as a function of the reduced volume, v. Note that lines of constant F are shown diagonally and are not orthogonal to lines of constant v. Stable shapes for the various volumes and their transition lines (dashed) are shown in the lower part. All shapes adhere to the substrate. The non-axisymmetric shapes have been calculated only at the marked points.

sure, $\Pi = k_B T(X_{ex} - N_{in}/V)$, vanishes up to a negligible contribution of the order of κ/R_0^3. In this case, an increase in the sugar content of the exterior fluid will raise i) the density of the exterior fluid directly, and ii) the density of the fluid enclosed in the vesicle by osmotically reducing its volume. The change of g with X_{ex} thus depends on experimental details. If $m_{in,\,ex}$ denotes the molecular masses of the sugars inside and outside the vesicle, one obtains

$$g = \frac{g_0 R_0^4}{\kappa}\left(\frac{N_{in}}{V} m_{in} - X_{ex} m_{ex}\right) \approx \frac{g_0 R_0^4 X_{ex}}{\kappa}(m_{in} - m_{ex}) \tag{4}$$

in the limit of small Π. Even the sign of the response of the density difference to the increase in sugar concentration, $\partial g/\partial X_{ex}$, depends on the types of sugars and the other osmotically active substances involved. It vanishes for $m_{in} = m_{ex}$. A trajectory starting at a point (g_s, v_s) will continue as $g(v) = g_s(v_s/v)$. Alternatively, one may vary only the density difference by *exchanging* sugars of different molecular weights in the exterior fluid, while keeping X_{ex} and the volume constant.

In conclusion, we have shown that additional energies are necessary for an experimentally realistic description of adhering vesicles. Gravity leads to non-axisymmetric shapes, which show continuous transitions to axisymmetric large-g shapes. For small volumes, the self-avoidance of the membrane and the associated self-adhesion energy lead to a large variety of «collapsed» shapes. By osmotic deflation or exchange of sugars it is possible to study these transitions with a single vesicle.

* * *

Stimulating discussions with F. JÜLICHER and W. WINTZ are gratefully acknowledged. We also thank H. G. DÖBEREINER, W. FENZL, J. RÄDLER and E. SACKMANN for sharing their knowledge on the experimental aspects of this work with us, and K. BRAKKE for help with Surface Evolver.

REFERENCES

[1] LIPOWSKY R. and SACKMANN E., *Structure and Dynamics of Membranes, Handbook of Biological Physics*, Vol. 1 (Elsevier Science, Amsterdam) 1995.
[2] EVANS E., *Colloids Surf.*, 43 (1990) 327.
[3] DÖBEREINER H.-G., PhD thesis, Simon Fraser University, Burnaby, Canada (1995).
[4] RÄDLER J. and SACKMANN E., *J. Phys. II*, 3 (1993) 727; RÄDLER J., FEDER T., STREY H. and SACKMANN E., *Phys. Rev. E*, 51 (1995) 4526.
[5] KRAUS M. and SEIFERT U., *J. Phys. II*, 4 (1994) 1117.
[6] SEIFERT U., *Phys. Rev. Lett.*, 74 (1995) 5060.
[7] HELFRICH W., *Z. Naturforsch. C*, 28 (1973) 693.
[8] DEULING H. and HELFRICH W., *J. Phys. (Paris)*, 37 (1976) 1335.
[9] SVETINA S. and ZEKS B., *Eur. Biophys. J.*, 17 (1989) 101.
[10] SEIFERT U., BERNDL K. and LIPOWSKY R., *Phys. Rev. A*, 44 (1991) 1182.
[11] MIAO L., SEIFERT U., WORTIS M. and DÖBEREINER H.-G., *Phys. Rev. E*, 49 (1994) 5389.
[12] SEIFERT U. and LIPOWSKY R., *Phys. Rev. A*, 42 (1990) 4768; LIPOWSKY R. and SEIFERT U., *Langmuir*, 7 (1991) 1867.
[13] SEIFERT U., *Phys. Rev. A*, 43 (1991) 6803.
[14] KRAUS M., SEIFERT U. and LIPOWSKY R., to be published.
[15] BRAKKE K., *Exper. Math.*, 1 (1992) 141. The Surface Evolver program is public domain and obtainable via anonymous ftp from geom.umn.edu in the /pub/software/evolver directory.
[16] NIKOLIC M., SEIFERT U., WINTZ W. and WORTIS M., submitted to *Phys. Rev. E*.
[17] MILNER S. and SAFRAN S., *Phys. Rev. A*, 36 (1987) 4371.
[18] SEIFERT U., *J. Phys. A*, 24 (1991) L573.